NANO LETTERS

2007
Vol. 7, No. 8
2365−2369

Bulk vs Nanoscale WS_2: Finite Size Effects and Solid-State Lubrication

S. Brown,[†,⊥] J. L. Musfeldt,*[,†] I. Mihut,[‡] J. B. Betts,[‡] A. Migliori,[‡] A. Zak,[§] and R. Tenne[||]

Department of Chemistry, University of Tennessee, Knoxville, Tennessee 37996, MPA-NHMFL, Los Alamos National Laboratory, Los Alamos, New Mexico 87545, NanoMaterials, Ltd., Weizman Science Park, Building 18, Nes Ziona 74140, Israel, and Department of Materials and Interfaces, Weizmann Institute of Science, Rehovot 76100, Israel

Received April 30, 2007

ABSTRACT

To investigate phonon confinement in nanoscale metal dichalcogenides, we measured the low-temperature specific heat of layered and nanoparticle WS_2. Below 9 K, the specific heat of the nanoparticles deviates from that of the bulk counterpart. Further, it deviates from the usual T^3 dependence below 4 K due to finite size effects that eliminate long wavelength acoustic phonons and interparticle-motion entropy. This separation of nanoscale effects from T^3 dependence can be modeled by assuming that the phonon density of states is flexible, changing with size and shape. We invoke relationships between the low-temperature T^3 phonon term, Young's modulus, and friction coefficient to assess the difference in the tribological properties. On the basis of this analysis, we conclude that the improved lubrication properties of the nanoparticles are extrinsic.

Nanomaterials offer fundamental new ways to explore strain, curvature, size, and shape effects on the physical properties of complex solids. Small length scales (and hierarchies of small length scales) dramatically alter the properties of nanoscale objects compared to their bulk counterparts, mandating a major revision of how we understand basic physical properties. This is especially true in the once-traditional field of thermodynamics, where high-precision heat capacity can provide direct information on the behavior of acoustic modes and hence quantum size effects in nanomaterials. In an ordinary three-dimensional insulating solid, the low-temperature specific heat, $C_p(T)$, increases as T^3. This is the well-known Debye model. Further, in an isolated, low-dimensional system, the low-temperature specific heat generally varies as T^D, where D is the dimensionality. In a nanomaterial, van Hove singularities and a hierarchy of important length scales can change dramatically these basic models.[1−3] For instance, summations over the quantized vibrational modes and peaks (or dips) in the phonon density of states that derive from dimensionality effects must be carried out explicitly to capture the contribution from both singularities and zeros. These modifications can have striking consequences for measurable thermodynamic quantities.[1,2]

Several intriguing examples of finite size effects in nanomaterials are beginning to emerge. For instance, the high aspect ratio of single-walled carbon nanotubes yields singularities in the phonon density of states, enhancing the specific heat of the nanotubes compared to that of graphite below 80 K.[2] A similar enhancement is observed in aligned multiwalled carbon nanotubes at a slightly lower energy scale.[4] Multiwalled TiO_2 nanotubes also display enhanced thermal properties compared to bulk anatase and rutile forms,[5] a result attributed to low-dimensional effects within an elastic continuum model. Thermal techniques have also been used to investigate bulk and nanoscale $CeCo_2$.[6] Here, confinement suppresses superconductivity and stabilizes (in its place) a low-temperature Kondo anomaly. These and other compounds provide exciting opportunities to examine finite length scale effects in complex solids.

MX_2 transition-metal dichalcogenides (where M is, for instance, Mo or W, and X is S or Se) are another set of materials where layered and various nanoanalogs exist.[7] Bulk $2H-WS_2$ consists of a sublayer of metal atoms sandwiched between two sublayers of sulfur, sharing the same $P6_3/mmc$ space group with graphite. This structure is locally preserved within the closed-caged nested nanoparticles,[8] referred to here as $IF-WS_2$ to emphasize their inorganic fullerene-like (IF) nature. Local symmetry-breaking effects caused by strain and

* Corresponding author. E-mail: musfeldt@utk.edu.
† Department of Chemistry, University of Tennessee.
‡ MPA-NHMFL, Los Alamos National Laboratory.
§ NanoMaterials, Ltd.
|| Department of Materials and Interfaces, Weizmann Institute of Science.
⊥ Presently at University College of London.

10.1021/nl0710147 CCC: $37.00
Published on Web 07/17/2007

curvature modify the bonding and change the local charging environment in the nanoparticles.[9] It is well-known that bulk transition-metal dichalcogenides are commonly used as commercial solid-state lubricants.[10] Recently, it has been reported that IF−WS_2 nanoparticles outperform traditional solid lubricants such as 2H−WS_2 and 2H−MoS_2 in many respects (friction, wear, and lubricant lifetime) under varied conditions.[11,12] Notably, the coefficient of friction of the nanoparticles is much smaller than that of the chemically identical but morphologically different bulk counterpart.

To investigate finite length scale effects in the nanoscale transition-metal dichalcogenides, we performed high-sensitivity specific heat measurements of both bulk and nanoparticle WS_2. We find that below 9 K, the specific heat of the nanoparticles deviates from that of the bulk counterpart. Further, it deviates from the usual T^3 dependence below 4 K. We discuss these differences in terms of vibrational confinement and interparticle-motion entropy. This separation of nanoscale effects from T^3 dependence can be modeled by assuming that the phonon density of states is flexible, changing with size and shape of the nanoparticle. Direct measurements of the lattice contribution to the specific heat also allow us to assess the intriguing mechanical and tribological properties of 2H− and IF−WS_2. On the basis of relationships between the low-temperature T^3 term, the Debye temperature, Young's modulus, and the friction coefficient, we conclude that the enhanced lubrication properties of the nanoparticles are extrinsic in origin.

IF−WS_2 was prepared from its oxide precursor, WO_3, following previously published procedures.[13] The nanoparticles of interest in this work are ∼120−200 nm in diameter. Bulk 2H−WS_2 was also used for comparison (Alfa Aesar, 99.8%). Isotropic pressed pellets were prepared to investigate the low-temperature thermodynamic properties. Typical surface qualities and pellet densities are given in ref 14. Both materials were vacuum annealed before pressing. The nanoparticles tend to aggregate into clusters ∼20−100 μm in sizes. These agglomerates usually decompose under pressure, for instance, during the pressure packing of nanoparticles.[14]

Specific heat measurements were carried out in a high-precision specific heat setup based on the semiadiabatic pulse relaxation method at Los Alamos National Laboratory between 0.3 and 30 K. Four independent measurements were taken at each temperature. Both warming and cooling responses were measured, and the resultant data sets were averaged. Temperature stability for each data point was better than ±2 mK. A close-up view of the measurement platform is shown in Figure 1. To avoid physadsorption of the N-grease, a thin layer of platinum was evaporated onto one side of the pellet before measurement.[15] The addenda and platinum film contributions[16] were subtracted to obtain the intrinsic specific heat of each sample. The high temperature thermal properties of both 2H− and IF−WS_2 were also investigated using a standard PPMS, with excellent agreement between the two measurements.

Figure 2 displays the low-temperature specific heat of 2H− and IF−WS_2 along with TEM images showing lattice

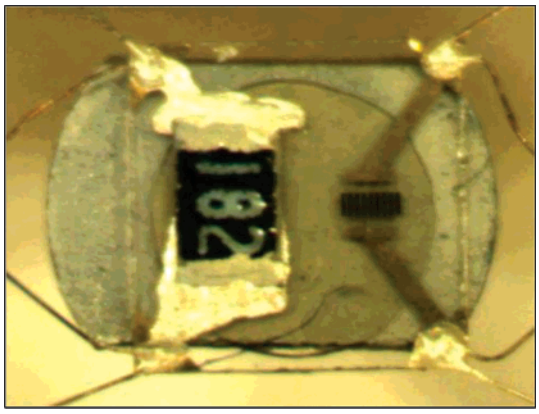

Figure 1. Close-up view of the underside of our specific heat apparatus. Here, the pressed pellet sample coated with a thin layer of platinum is mounted on the experimental platform with N-grease. The sapphire platform is equipped with a heater and temperature sensor and is well-isolated from the environment.

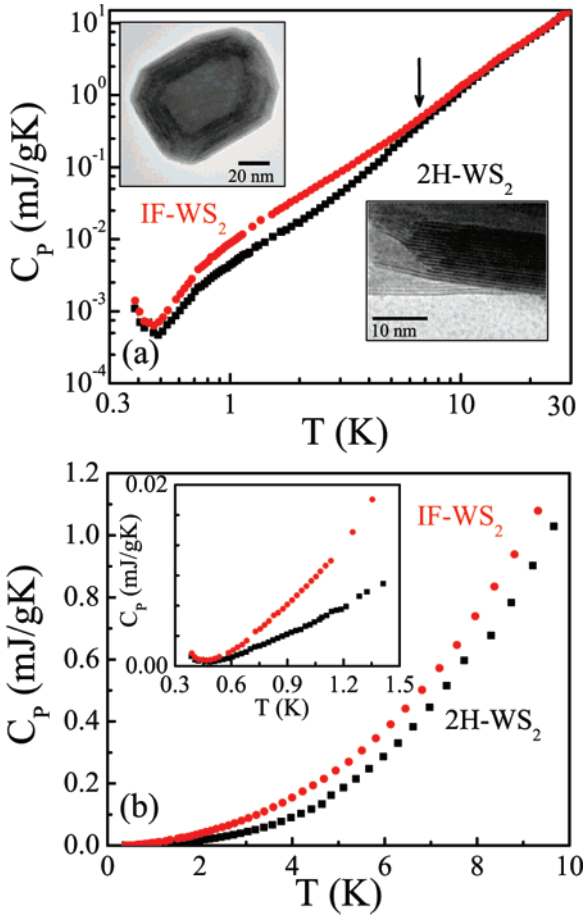

Figure 2. (a) Specific heat of 2H− and IF−WS_2 as a function of temperature. Transmission electron microscope images are shown to emphasize the bulk layered vs nanoscale morphologies. (b) Low-temperature specific heat of 2H− and IF−WS_2 on a linear scale. The inset shows a close-up view of the data below 1.5 K. The error bars are smaller than the symbol size.

fringing for the layered bulk and the nested character of the nanoparticles. The high-temperature response (above 10 K) is similar for both materials, as expected. Below 9 K, the specific heat of the nanoparticles deviates from that of the bulk counterpart. This non-Debye-like change in slope

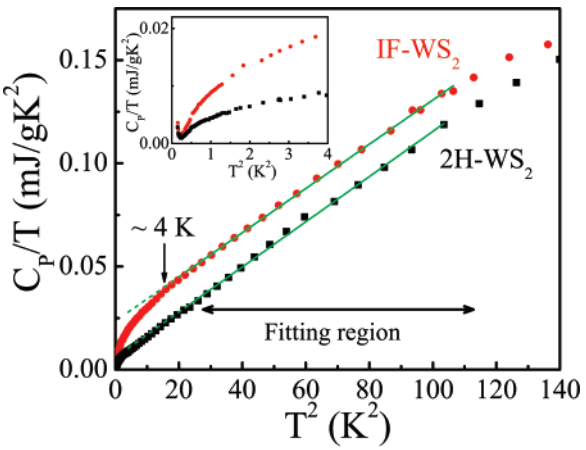

Figure 3. C_p/T vs T^2 plot for 2H− and IF−WS_2 along with a best-fit straight line (green dashed) in the low-temperature linear range. The inset shows a close-up view of the low-temperature trend for both materials, emphasizing the non-Debye character of C_p/T for the nested nanoparticles below 4 K.

reflects the freezing out of internal modes, as discussed below. The specific heat of IF−WS_2 is enhanced compared to that of the bulk counterpart. At very low temperatures (below 0.6 K), there is an upturn in the thermal response of both materials.

It is interesting to compare the thermodynamic properties of bulk and nanoscale metal dichalcogenides (Figure 2) with specific heat measurements of other model materials. Overall, these studies show that bulk and nanotube specific heats are similar at high temperatures, while at low temperature, the specific heat of the nanomaterial is enhanced compared to that of the layered parent compound. The degree of enhancement and the energy scale for the effect depend upon the physical system. For instance, single- and multiwalled carbon nanotubes show an especially large increase in specific heat compared to graphite below 100 K, a result that derives from dimensional crossover effects and singularities in the phonon density of states of the tubular materials.[2,4] An extra T^{α} term, attributed to localized low-energy excitations, is also reported in single-walled carbon nanotube bundles.[17,18] Similarly, the specific heat of multiwalled TiO_2 nanotubes exhibits a large enhancement compared to bulk anatase and rutile forms below 50 K.[5] This deviation is attributed to differences in the low-temperature density of states of the acoustic phonons.

To quantify the differences in the specific heat of 2H− and IF−WS_2 and compare our results with the well-known Debye model, we plotted C_p/T vs T^2 and fit our results according to

$$C_p/T = \gamma + \alpha T^2 \qquad (1)$$

Here, γ represents the electronic specific heat, and the coefficient α captures the lattice specific heat contribution. These results are shown in Figure 3. Below 10 K, the thermal response of 2H−WS_2 follows eq 1 quite well, and it is linear down to 1.5 K. In contrast, IF−WS_2 exhibits linear behavior only in a limited temperature range (∼4−10 K). Below 4 K, the specific heat of IF−WS_2 deviates strongly from the traditional Debye model and the associated T^3 dependence. This deviation from linearity in the C_p/T vs T^2 plot is attributed to finite size effects in the WS_2 nanoparticles, as discussed below. A similar deviation from T^3 dependence is observed in carbon and TiO_2 nanotubes,[2,4,5] although the energy scale for the appearance of quantum size effects in the transition metal dichalcogenide nanoparticles is much less than that reported for the tubular materials.

Of course, the character of acoustic mode dispersion in the Debye model (and the abandonment of dispersion entirely in the Einstein model) provides only the crudest framework from which to understand the low-temperature thermodynamic properties of insulating solids where nanometer length scales modify the bulk near-continuum phonon density of states. For our study, there are three key departures from the simplest bulk-continuum model, best seen in a plot of C_p/T vs T^2 (Figure 3). They are: (1) at some low temperature, C_p/T drops below the linear-in-T^2 fit, (2) there is a clear minimum, and (3) at the lowest temperatures, C_p/T vs T^2 increases as $1/T$. An approximation still, but which includes all the essential physics of this problem and which reproduces the three key features of the low-temperature specific heat measurement, can be constructed as follows. Consider that the compressed nanoscale powder consists of, say, n spheres, each containing m atoms. We can separate the contributions to the heat capacity into two components. One component is simply the heat capacity of n separate, noninteracting nanoparticle spheres of m atoms. Each sphere has $3m - 3$ internal modes. n such spheres have $n(3m - 3) = 3nm - 3n$ modes. However, the total number of vibrational modes must be $3nm - 3$, leaving $3n - 3$ modes unaccounted for. The other component contains these missing $3n - 3$ modes. Here is how. Because the individual spheres at temperatures well below our measurement temperature have no accessible internal degrees of freedom but are elastically connected via weak springlike forces,[19] they act like a simple mass-spring solid but now with masses of order 10^6 an atomic mass (the mass of each nanoparticle). Thus the compressed solid at temperatures too low to excite the internal modes of the nanoparticles (less than 0.1 K) behaves like a solid of n particles with a Debye temperature that is many orders of magnitude lower than that for ordinary solids. At temperatures well below the measurements made here, all the interparticle modes can be thermally occupied, much like an ordinary solid above the Debye temperature. Such a solid has heat capacity of $3k_b$/mode, independent of temperature like the Dulong and Petite high-T limit in a conventional solid for a total heat capacity of

$$C_p = 3k_b(n - 1) \qquad (2)$$

To this we now must compute and add, reasonably accurately, the heat capacity of the internal modes of the spheres to obtain the total heat capacity. Although the codes we use to analyze resonant ultrasound spectroscopy studies[20] can be used to compute the exact modes up to several thousand in number, the differences are very small compared to the simple periodic boundary-condition problem for plane

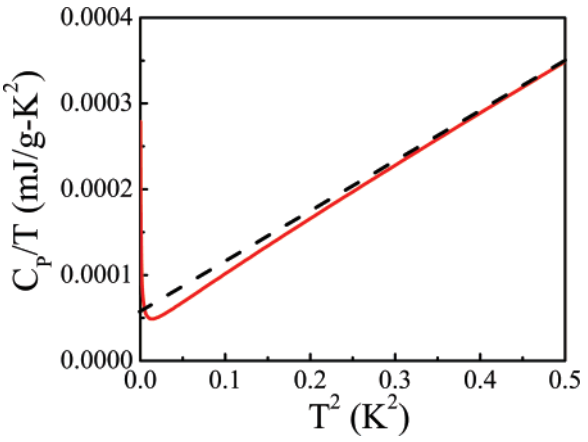

Figure 4. Model calculation using a heat capacity that is the sum of interparticle and intraparticle contributions (eq 2 and the derivative of the energy in eq 3), employing reasonable values of shear and longitudinal moduli and for cubes whose edge is about the same as the central peak in the size distribution of the nanoparticles measured here. Here, the red solid line is the simulated thermal response of the nanoparticles. The dashed black line shows typical T^3 dependence and shows where the approximations converge on the bulk results.

waves. For an isotropic cube (the differences between cube, sphere, and the actual layered not-quite-spherical particles we measured are very small and beyond the scope of this study), the plane-wave boundary conditions are on the *k*-vectors of the modes. For a cube with 3 modes/unit cell and *m* unit cells of lattice parameter *a*, the linear dimensions are $l_1 = l_2 = l_3 = am^{1/3}$. Then $k_{i,j} = 2\pi/(2l_i/j)$ where $i = x$, y, or z directions, j is the mode index, and we are fitting integral numbers of half-wavelengths into the cube. Let us also assume just one type of dispersion curve, say shear, to simplify things. Then if the shear wave speed is c, the total internal vibrational energy at a suitably low-temperature T can be approximated by

$$E = \frac{\hbar\pi c}{am^{1/3}} \sum_{i,j,l=1}^{\infty} \frac{[i^2 + j^2 + l^2]^{1/2}}{e^{E_{i,j,l}/k_B T} - 1} \tag{3}$$

where

$$E_{i,j,l} = \frac{\hbar\pi c}{am^{1/3}}[i^2 + j^2 + l^2]^{1/2} \tag{4}$$

The intraparticle heat capacity is then the derivative of the energy (eq 3) with respect to the temperature.

The critical difference between this sum in eq 3 and the usual Debye approximation is that there is a hole in the phonon mode distribution because there is a now a lowest mode. The radius of the hole is $\hbar\pi c/am^{1/3}$. It is this hole that is going to produce most of the low-temperature physics for the problem. Summing the interparticle and intraparticle contributions to the heat capacity (eq 2 and the derivative of the energy in eq 3), we compute the specific heat and show the result in Figure 4. This calculation used a longitudinal modulus of 180 GPa, a shear modulus of 60 GPa, a density of 7400 Kgm^{-3} and a cube edge of 140 nm. The numerical computation used both the shear and longitudinal moduli rather than just the shear modulus as in eq 3. Note that all the salient features of our measurement are reproduced—the departure from T^3, the low-T minimum, and the very low-T upturn. The key temperature scale is that of the lowest internal shear mode and is about 0.5 K. It is not very useful to attempt to do a more exact computation than this because many of the parameters are not measurable by us, such as the degree of compression of the powder, the actual shape and size distribution, surface modifications to the internal modes from nanoscale effects,[3] and more.

Can we use the data in Figure 3 to understand and assess the relative tribological properties of bulk and nanoscale transition-metal dichalcogenides? A simple physical argument can indeed capture much of the essential physics. We can extract the Debye temperature, θ_D, for both 2H− and IF−WS_2 from the slope of the C_p/T vs T^2 plot in the region where low-temperature specific heat follows T^3 behavior as

$$\theta_D = (12\pi^4 R/5\alpha)^{1/3} \tag{5}$$

Here, R is the gas constant. Note that in evaluating the slope, we avoided both the extreme low-temperature regime and also $T \geq 20$ K, where the Debye T^3 approximation becomes poor. The Debye temperature is directly related to Young's modulus (which is a measure of stiffness) as

$$\theta_D \sim \sqrt{\frac{Y}{\rho}} n^{1/3} \sim \sqrt{\frac{Y}{M}} \tag{6}$$

Here, Y is Young's modulus and M the mass (using $\rho = nM$).[21] We focus on the mass relation in eq 6 because density is difficult to measure in a nanomaterial[14,22] and we do not know the number of moles. Further, θ_D is the characteristic temperature at which all modes are excited in a material, and it is the number of modes that matters. Hence, stiffer materials and smaller M are associated with higher θ_D. Recently, Tambe and Bhushan discovered that the coefficient of friction, f, goes as $1/Y$ for a wide variety of materials.[23] Direct AFM studies of nanoscopic sliding friction on CrN thin films with varying hardnesses grown at different temperatures also demonstrates that changes in the friction coefficient derive from variations in the Young's modulus.[24] This relationship ($f \sim 1/Y$) has not been tested for nanomaterials, but it is anticipated to hold.[25] Together, these relationships provide a direct link between the thermodynamic, mechanical, and tribological properties of a material, and we can employ them to evaluate the relative friction coefficients in 2H− and IF−WS_2.

As shown in Figure 3, the slopes extracted from the linear range of the C_p/T vs T^2 data are very similar for both compounds. This implies nearly identical Debye temperatures, Young's moduli, and coefficients of friction.[26] This analysis suggests that the substantially improved coefficient of friction in IF−WS_2 does not derive from the unique nanoscale architecture and is not intrinsic. The improved

lubrication characteristics of the nanoparticles compared with the bulk must therefore be attributed to some extrinsic mechanism. The puncturing/deformation/delamination of the nanoparticles and "filling-the-gaps" processes should therefore be examined in greater detail.[27] Recent density-functional tight-binding-based molecular dynamics calculations on WS_2 nanotubes suggest that platelets may form upon rupture, optimally located in grooves or parallel to contact surfaces.[28] Work on ZnS nanorods also shows that the best solid-state lubrication properties are obtained when multiple layers are trapped between surfaces.[29]

To summarize, we measured the low-temperature specific heat of layered and nanoparticle WS_2 to investigate finite length scale effects in two chemically identical but morphologically different transition-metal dichalcogenides. Below 9 K, the specific heat of the nanoparticles deviates from that of the bulk counterpart. The enhanced specific heat of the nanoparticles is consistent with recent results on carbon and TiO_2 nanotubes.[2,4,5] Further, the specific heat of IF−WS_2 deviates from the usual T^3 dependence below 4 K because of the suppression of long wavelength acoustic modes due to finite size effects and interparticle-motion entropy. This separation of nanoscale effects from T^3 dependence can be modeled by assuming that the phonon density of states is flexible, changing with size and shape of the nanoparticle. We reproduce all the unusual low-temperature specific heat deviations from a Debye model with a simple semi-exact computation of heat capacity in which nanosize effects block out a hole in the distribution of phonons around zero frequency, providing a mechanism for freezing out of internal vibrational heat capacity as spectral weight shifts from the hole to a very low-temperature interparticle Debye-like behavior. We also employ the low-temperature specific heat data of 2H− and IF−WS_2 and a simple physical argument to assess the mechanical and tribological properties of these materials. On the basis of this analysis, we conclude that the improved solid-state lubrication properties of the nanoparticles are extrinsic, that is, not related to the elastic properties of the particles but possibly derived from particle positioning or delamination effects at friction contact points.

Acknowledgment. Work at the University of Tennessee is supported by the Materials Science Division, Office of Basic Energy Sciences at the U.S. Department of Energy under grant no. (DE-FG02-01ER45885). A portion of this research was performed under the auspices of the National Science Foundation, the State of Florida, and the U.S. Department of Energy. Work at the Weizmann Institute of Science is supported by the Helen and Martin Kimmel Center for Nanoscale Science and by NanoMaterials, Ltd. R.T. is the holder of the Drake Family Chair in Nanotechnology. We thank Shiliang Li for assistance with early PPMS work and Ronit Popovitz-Biro for the transmission electron microscope images.

References

(1) Allen, K.; Hellman, F. *Phys. Rev. B* **1999**, *60*, 11765.
(2) Hone, J.; Batlogg, B.; Benes, Z.; Johnson, A. T.; Fischer, J. E. *Science* **2000**, *289*, 1730.
(3) Nagy, T. F.; Conley, J. J.; Tománek, D. *Phys. Rev. B* **1994**, *50*, 12207.
(4) Masarapu, C.; Henry, L. L.; Wei, B. *Nanotechnology* **2005**, *16*, 1490.
(5) Dames, C.; Poudel, B.; Wang, W. Z.; Huang, J. Y.; Ren, Z. F.; Sun, Y.; Oh, J. I.; Opeil, C.; Naughton, M. J.; Chen, G. *Appl. Phys. Lett.* **2005**, *87*, 031901.
(6) Chen, Y. Y.; Jang, S.-J.; Wang, C. R.; Yang, H. D. *Physica B* **2005**, *359*, 497.
(7) Tenne, R. *Nat. Nanotechnol.* **2006**, *1*, 103.
(8) Feldman, Y.; Frey, G. L.; Homyonfer, M.; Lyakhovitskaya, V.; Margulis, L.; Cohen, H.; Hodes, G.; Hutchison, J. L.; Tenne, R. *J. Am. Chem. Soc.* **1996**, *118*, 5362.
(9) Luttrell, R. D.; Brown, S.; Cao, J.; Musfeldt, J. L.; Rosentsveig, R.; Tenne, R. *Phys. Rev. B* **2006**, *73*, 035410.
(10) Solid-state lubrication extends the operating conditions of sliding systems beyond 300 K to high-vacuum, high-temperature, cryogenic-temperature, radiation, space, or corrosive environments.
(11) Rapoport, L.; Bilik, Yu.; Feldman, Y.; Homyonfer, M.; Cohen, S. R.; Tenne, R. *Nature* **1997**, *387*, 791.
(12) Kaplan-Ashiri, I.; Cohen, S. R.; Gartsman, K.; Ivanovskaya, V.; Heine, T.; Seifert, G.; Wiesel, I.; Wagner, H. D.; Tenne, R. *Proc. Natl. Acad. Sci. U.S.A.* **2006**, *103*, 523.
(13) Tenne, R.; Margulis, L.; Genut, M.; Hodes, G. *Nature* **1992**, *360*, 444.
(14) Kopnov, F.; Yoffe, A.; Leitus, G.; Tenne, R. *Phys. Status Solidi B* **2006**, *243*, 1229.
(15) Both 2H− and IF−WS_2 showed showed strong absorption of N-grease, resulting in a modified thermal response below 10 K. We speculate that the grease might "fill the gaps" between platelets or particles, increasing interparticle interactions. A thin coating of Pt was used to prevent physadsorption in our samples.
(16) Martin, D. L. *Phys. Rev. B* **1978**, *17*, 1670.
(17) Lasjaunias, J. C.; Biljakovi, K.; Benes, Z.; Fischer, J. E.; Monceau, P. *Phys. Rev. B* **2002**, *65*, 113409.
(18) Lasjaunias, J. C.; Biljakovic, K.; Monceau, P.; Sauvajol, J. L. *Nanotechnology* **2003**, *14*, 998.
(19) Landau, L. D.; Lifshitz, E. M. *Theory of Elasticity*, 3 rd ed.; Pergamon Press: London, 1986.
(20) Migliori, A.; Maynard, J. D. *Rev. Sci. Instrum.* **2005**, *76*, 1.
(21) Omar, M. A. *Elementary Solid State Physics: Principles and Applications*; Addison Wesley: Berkeley, CA, 1999.
(22) It is very difficult to measure density of a nanomaterial anyway due to physabsorption and chemabsorption effects.
(23) Tambe, N. S.; Bhushan, B. *Appl. Phys. Lett.* **2005**, *86*, 061906.
(24) Riedo, E.; Brune, H. *Appl. Phys. Lett.* **2003**, *83*, 1986.
(25) Bushan, B. private communication.
(26) From the slope, we find $\Theta_D \sim 191$ K for both materials and a Young's modulus that displays order of magnitude agreement with direct measurements in the scanning electron microscope ref 12.
(27) Rapoport, L.; Fleischer, N.; Tenne, R. *J. Mater. Chem.* **2005**, *15*, 1782.
(28) Enyashin, A. ; St. Steganov, M.; Heine, T.; Seifert, G. in preparation.
(29) Akbulut, M.; Belman, N.; Golan, Y.; Isrealachvili, J. *Adv. Mater.* **2006**, *18*, 2589.

NL0710147